Twenty-Seventh Symposium (International) on Combustion/The Combustion Institute, 1998/pp. 469–476

ABSOLUTE RADICAL CONCENTRATION MEASUREMENTS AND MODELING OF LOW-PRESSURE CH_4/O_2/NO FLAMES

W. JUCHMANN,[1] H. LATZEL,[1] D. I. SHIN,[1] G. PEITER,[1] T. DREIER,[1] H.-R VOLPP,[1] J. WOLFRUM,[1] R. P. LINDSTEDT[2] AND K. M. LEUNG[2]

[1]*Physikalisch Chemisches Institut*
Universität Heidelberg
Im Neuenheimer Feld 253
D-69120 Heidelberg, Germany
[2]*Department of Mechanical Engineering*
Imperial College of Science, Technology and Medicine
Exhibition Road
London SW7 2BX, UK

An experimental and theoretical investigation of CH and CN radical formation and destruction in a low-pressure 13.3-hPa (10 Torr) premixed stoichiometric CH_4/O_2 flame seeded with NO is presented. Relative concentration profiles of CH and CN are measured by linear unsaturated laser-induced fluorescence (LIF). An absolute calibration of the relative profiles is obtained by Rayleigh scattering. A computational study is performed to identify key uncertainties in the formation and destruction chemistry of the CH and CN radicals. It is shown that the reaction of the CH radical with molecular oxygen is of particular importance in the present flame. Prevailing uncertainties in the reactions of $^3CH_2$ with hydrogen atoms and molecular oxygen are also discussed. The present quantitative measurements of the CN radical also indicate that further attention should be given to the formation and oxidation chemistry of HCN. Nevertheless, computational results are encouraging and reasonable agreement is obtained for both the CH and CN radicals. It is further shown that the effects on CH concentration levels of introducing NO dopants may be reproduced. Comparisons of absolute concentration profiles of CH_3, OH, and CH radicals as well as NO are also made with computed results obtained using GRI Mech. 2.11 and a reaction mechanism developed by Warnatz. The computations highlight significant differences in reaction paths and rate selection. The major areas of uncertainty are outlined and tentative recommendations are made in relation to the key reaction paths.

Introduction

In recent years, the formation and destruction of nitrogen oxides in flames have been extensively studied experimentally [1–7] and theoretically [8–10]. The studies performed have provided an understanding of the interaction of hydrocarbon radicals and nitrogen-containing species involved in the NO formation and removal ("reburn process") chemistry. Several reaction mechanisms have been developed and successfully applied to the modeling of spatial profiles of intermediate species [8–10]. However, significant uncertainties still prevail in the rate coefficients and product distributions of a number of key reactions involving the formation and destruction of free radicals. Relative radical concentration measurements of intermediate species obtained using laser-induced fluorescence (LIF) [6,7] have the potential to facilitate the development of detailed reaction mechanisms capable of reproducing qualitative trends across a wide range of fuels. However, the lack of quantitative measurements of key radical species renders it difficult for any modeling effort to resolve the uncertainties associated with absolute concentration levels. The need to provide quantitative predictions of intermediate species responsible for the formation of pollutants is self-evident. The situation with respect to quantitative determinations of key radical species has been improved by recent experiments using laser absorption, degenerate four-wave mixing, and LIF, which have provided quantitative measurements of CH_3 [11,12], OH [11], and CH [13] radicals. The situation with respect to the CH radical is particularly encouraging in view of its predominant role in the "prompt" NO formation mechanism. In this paper, absolute CH and CN concentrations are determined *in situ* by calibrated LIF measurements. The experimental data are compared with the results of flame structure calculations in an effort to quantify the uncertainties of current kinetic models with regard to the formation and destruction chemistry of the CH and CN radicals. The flame considered in this work is particularly well suited to illustrate difficulties related to the balancing of

hydrogen abstraction and molecular oxygen reactions. The major uncertainties concerning the controlling fundamental rate constants are outlined, and it is shown that reasonable agreement may be obtained through the use of reaction rate parameters well within accepted experimental uncertainty limits.

Experimental Configuration

Measurements have been performed in a low-pressure 13.3-hPa (10 Torr) stoichiometric CH_4/O_2 flame stabilized on a McKenna- (flat porous plate) type burner. The burner facility has been described in detail by Etzkorn et al. [3] and the temperature profile, also determined in previous work using OH LIF, is used in the present study. Doped flames have been studied through the addition of a small amount of nitric oxide (1.8% of the total gas flow) through a separate mass flow controller. For species and temperature determination, LIF detection as well as Rayleigh calibration measurements [13–15] of CH and CN were performed. The experimental setup for the LIF excitation and detection is identical with the one by Selle and Monkhouse [14] and features tunable radiation around 387 nm originating from a narrowband dye laser (Lambda Physik, Scanmate, 5 mJ in a 12-ns pulse) pumped by a XeCl excimer laser (80 mJ/pulse, 10-Hz repetition rate), which is passed unfocused (1-mm diameter) through the flame. Using Quinolon dye dissolved in dioxane, the laser beam energy was varied by neutral density filters, dichroic mirrors, and an iris in front of the entrance window of the burner housing. The pulse energy is monitored continuously with a pyroelectric joulemeter (Laser Probe) behind the exit window. The laser pulses have a spectral bandwidth of 0.25 ± 0.03 cm^{-1} at 388 nm as measured with a monitor etalon. LIF and Rayleigh signals from the probe volume are imaged onto the entrance slit of a 0.5-m monochromator (CVI, Digikrom 480) and detected by a photomultiplier (Hamamatsu, R4332) behind the exit slit. To capture all broad-band fluorescence light after excitation, the grating was used in 0th order with a Schott filter combination (WG 335 + BG 3) in front of the entrance slit, for most of the measurements. For time-integrated intensity measurements and the determination of fluorescence lifetimes, the signal from the photomultiplier (PMT) was fed into a gated integrator (SRS 250) and a digital storage oscilloscope (LeCroy 9350A, 500 MHz), respectively.

Measurement Procedure

For comparison with the simulations, the following parameters were obtained experimentally: (1) temperatures determined from relative LIF intensity ratios of several CH transitions at selected positions above the burner; (2) relative CH and CN concentration profiles along the centerline of the burner, and (3) calibration of relative concentration profiles by the Rayleigh calibration method described by Luque et al. [15]. To verify the temperature profile in the present flame (as taken from the previous work [3]), temperatures were determined at a few locations from a Boltzmann plot of selected and isolated transitions excited in the R-branch of the CH B-X (0,0) electronic band system. Closely spaced rotational transitions with rotational quantum numbers J between 4 and 10 for both spin states were chosen from LIF excitation scans (Fig. 1). With the laser energy in the linear regime (<1 μJ), the CH rotational temperatures in the present work agree within the error limits with the previous results. Linear unsaturated LIF has been used to determine the signal intensity as a function of height above the burner. In this case the relationship between the detected signal S_F and the molecular concentration N is given by [15]

$$S_F = N f_B \frac{B}{c} E_L \frac{\Gamma}{\Delta\nu} \frac{\tau_{eff}}{\tau_0} \frac{g}{4\pi} \qquad (1)$$

where f_B is the Boltzmann factor, B the absorption coefficient for the excited rotational transition, E_L is the laser energy, Γ the line shape overlap, $\Delta\nu$ the laser bandwidth, and g a function of the optical collection and transmission efficiency. To determine absolute number densities from the LIF signal, the effective lifetime τ_{eff}, that is, the fluorescence quantum yield τ_{eff}/τ_0, has to be determined. This was done by direct measurement of the total fluorescence decay time of the excited transitions as a function of position in the flame to account for the specific collisional quenching environment. The remaining unknown factor g was determined from the slope of the Rayleigh scattering signal intensity S_R (Fig. 2) as a function of the product of number density N of nitrogen and laser energy E_L [15]:

$$S_R = N \frac{E_L}{hc\nu} \left(\frac{\partial\sigma}{\partial\Omega}\right) g \qquad (2)$$

Excitation and detection geometry, filter selection, and electronic settings of the PMT/gated integrator are kept the same as in the LIF measurements. For absolute calibrations, the $R_1(9)$ and $R_1(12)$ transitions of CH at 387.42 and 388.15 nm were selected. The CN calibration was performed using the $P_{1,2}(10)$ transition at 388.11 nm. For the determination of concentration profiles of CH, the $R_1(9)$ line was used. For CN, relative LIF intensity profiles taken from transitions of the unresolved P(0,0) bandhead at 388.44 nm were compared with profiles taken with the $P_{1,2}(10)$ line. The comparison showed no difference within the error limits, and therefore

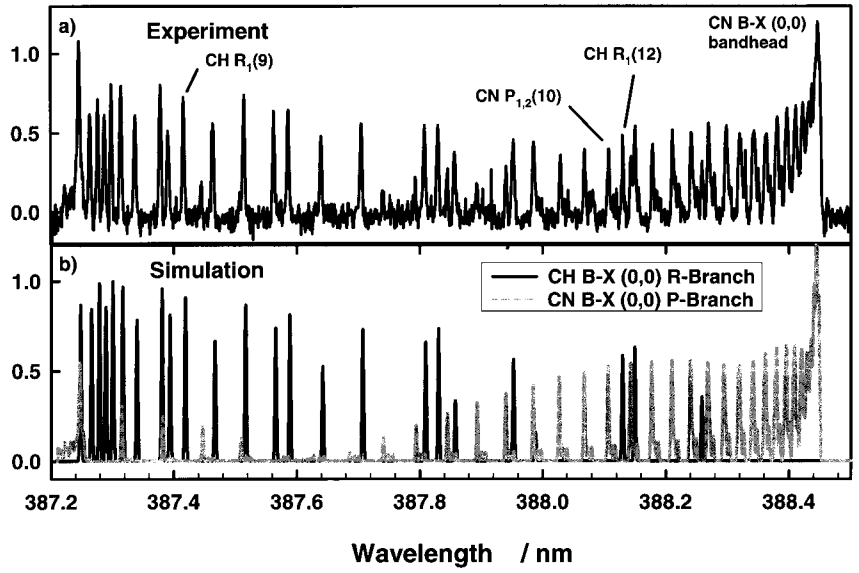

FIG. 1. (a) LIF excitation scan of CH B-X and CN B-X in the low-pressure (13.3-hPa) flat flame (CH_4:O_2/ 1.33:2.66 slm) with seeded NO (0.072 slm) at $z = 5$ mm from the burner surface; (b) simulation of CH B-X (black) and CN B-X (gray) spectra at $T = 2000$ K in the same spectral region (Ref. [16]).

the bandhead was chosen to obtain a better signal-to-noise ratio.

Detailed Kinetic Modeling

The flame structure is modeled by solving the conservation equations for a laminar premixed burner-stabilized flame [17] with the experimental temperature profile, volumetric flow rate (4.0 slm), and reactant composition imposed upon the computation. Three different detailed chemical kinetic reaction mechanisms are compared in this work. The first is identical to that applied by Sick et al. [18] in their modeling of NO formation and destruction in counterflow diffusion flames. This mechanism is based on the work of Lindstedt and coworkers [10,19,20], and it has subsequently been updated to include more recent kinetic data. Changes relevant to this work are outlined in Table 1. GRI-Mech. 2.11 [9] and the reaction mechanism of Warnatz et al. [31] are also applied to model the present flame.

An analysis of the three mechanisms reveals significant differences with respect to key reaction paths. The model of Lindstedt and coworkers features a rate for the $^3CH_2 + O_2$ reaction based on the work of Dombrowsky and Wagner [21]. The determined rate is in excess of one order of magnitude slower at a temperature of 1800 K than the rates used in the other mechanisms [9,31]. Further differences can be found in the rate constants for the $^3CH_2 + H = CH + H_2$ reaction. There are substantial uncertainties with respect to this reaction,

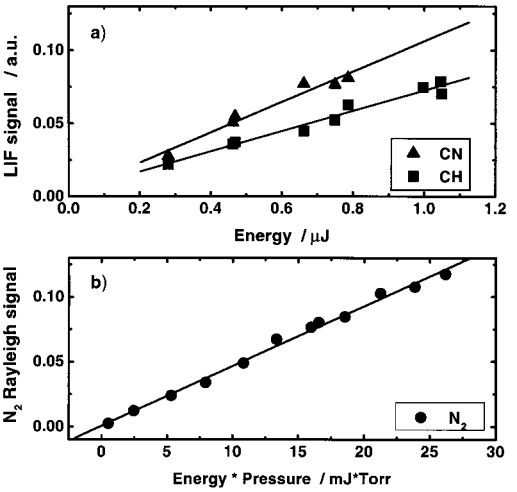

FIG. 2. (a) LIF signal intensity versus laser energy from the excited CH B-X $R_1(12)$ (▲) and the excited CN B-X $P_{1,2}(10)$ lines (■); (b) calibration of the detection system by Rayleigh scattering.

and estimates range from 8.0×10^9 m^3/kmol s [33] to more than 5.0×10^{11} m^3/kmol s [34] at temperatures above 2000 K. The recent work of Röhrig et al. [35] has deduced limiting rates of 3.2×10^{10} m^3/kmol s and 2.3×10^{11} m^3/kmol s in the temperature range of 2200–2600 K. The present mechanism features a temperature independent rate of 1.1×10^{11}

TABLE 1
Rate coefficients in the form $k = AT^n \exp(-E/RT)$

Reaction	A (m^3/kmol × s)	n	E (kJ/mol)	Ref.
$^3HC_2 + H = CH + H_2$	1.100E+11	0.00	0.00	[22]
$^3CH_2 + O_2 =$ Product	3.324E+19	−3.30	12.00	[19,21]
$CH + O_2 = CHO + O$	7.500E+10	0.00	0.00	[23]
$CH + H = C + H_2$	3.000E+10	0.00	0.00	[24]
$C + O_2 = CO + O$	1.200E+11	0.00	16.71	[25]
$NO + C = CN + O$	2.000E+10	0.00	0.00	[10]
$NO + C = N + CO$	2.800E+10	0.00	0.00	[10]
$NO + CH = HCN + O$	4.800E+10	0.00	0.00	[26]
$NO + CH = NCO + H$	1.800E+10	0.00	0.00	[26]
$NO + CH = CHO + N$	2.600E+10	0.00	0.00	[26]
$NO + CH = NH + CO$	5.000E+09	0.00	0.00	[26]
$NO + CH = CN + OH$	3.000E+09	0.00	0.00	[26]
$NO + {}^3CH_2 = HCNO + H$	2.500E+09	0.00	25.00	[27]
$NO + {}^3CH_2 = HCN + OH$	5.000E+08	0.00	12.00	[27]
$NO + {}^1CH_2 = HCNO + H$	6.600E+09	0.00	0.00	Est.
$NO + {}^1CH_2 = HCN + OH$	3.400E+09	0.00	0.00	Est.
$HCN + O = NH + CO$	5.400E+05	1.21	31.34	[28]
$HCN + O = NCO + H$	2.000E+05	1.47	31.76	[28]
$HCN + O = CN + OH$	4.200E+07	0.40	86.50	[26]
$HCN + OH = CN + H_2O$	3.900E+03	1.83	43.00	[29]
$CN + O = CO + N$	7.700E+10	0.00	0.00	[30]
$CN + OH = NCO + H$	6.000E+10	0.00	0.00	[10]
$CN + O_2 = NCO + O$	6.620E+09	0.00	−1.70	[10]

m^3/kmol s based on the determination of Böhland and Temps [22]. The rate used in GRI-Mech. 2.11 was obtained by reducing the upper limit expression of Zabarnick et al. [34] by a factor of three. The rates adopted in GRI-Mech. 2.11 and the present mechanism are thus fairly close to the median value suggested by Röhrig et al. [35]. By contrast, the rate expression adopted by Warnatz et al. [31] is close to the lower limit [33] at combustion temperatures. A third major difference is related to the reactions of CH with O_2 and H_2O. GRI-Mech. 2.11 and the Warnatz mechanism adopt the Commission of the European Communities (CEC) recommendation [32] of 3.3×10^{10} m^3/kmol s for the $CH + O_2$ reaction. This rate is close to the room-temperature determination of Berman et al. [36]. However, Markus et al. [23] investigated the same reaction at high temperatures (2500–3500 K) and obtained a rate constant of 7.5×10^{10} m^3/kmol s, which is used in the present mechanism. This higher value has recently been given support by the study of Röhrig et al. [35], who obtained a value of 9.7×10^{10} m^3/kmol-s (2200–2600 K). The reaction between CH and H_2O is also a potentially major sink for the CH radical. The mechanism of Lindstedt and coworkers features a rate expression adopted from Baulch et al. [32] with the product specified as an adduct (CH_2OH). The same total rate expression is used by Warnatz. However, two product channels ($CH_2O + H$ and $^3CH_2 + OH$) are specified with a branching ratio of 4:1. GRI-Mech. 2.11 is based on the same source with a single product channel ($CH_2O + H$). However, the rate constant is assigned a value three times higher than the CEC recommendation [32].

Reactions between C_1 hydrocarbon radicals and NO are mainly responsible for "reburn" in the present flame, and the computed CN concentration is sensitive to the rates and product distribution of these reactions. GRI-Mech. 2.11 and the present mechanism feature rate constants and product distributions for the reactions of NO with C and CH obtained from the work of Dean et al. [37] and Dean and Bozzelli [26]. The mechanism of Warnatz exclusively considers CN and HCN as products for the reactions of NO with C and CH. However, both the present and Warnatz mechanisms adopt the rate constant and product distribution for the $NO + {}^3CH_2$ reaction from the work of Bauerle et al. [27]. The total rate suggested in Ref. [27] is ~10 times slower at 1800 K than that used in GRI-Mech. 2.11. Hydrogen cyanide is a major product of the NO reburn chemistry, and its subsequent reactions with H, O, and OH radicals lead to the formation of CN, NCO, and NH radicals. Glarborg and Miller [38]

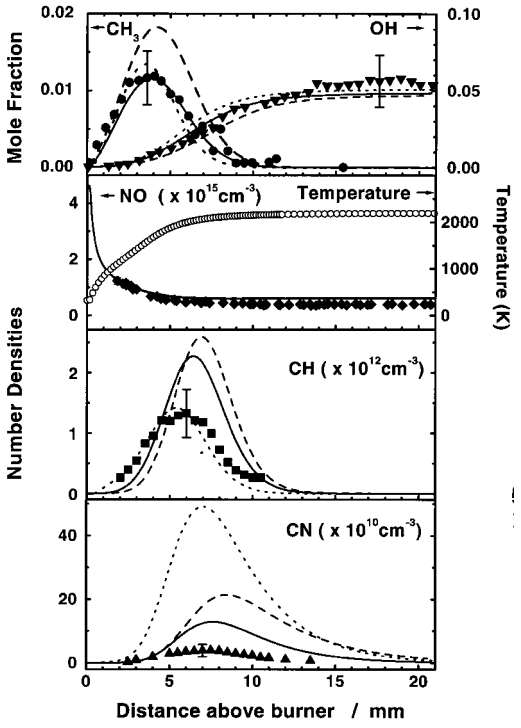

FIG. 3. Measured OH (▼), CH_3 (●), NO (◆), CH (■), and CN (▲) absolute concentration profiles in the 13.3-hPa (10-Torr) (CH_4/O_2/NO flame. Comparison with results from chemical kinetics modeling using reaction mechanism from present work (—), the GRI 2.11 (---) (Ref. [19]), and Warnatz mechanism (. . .) (Ref. [31]). The given experimental error for CH and CN represents 2σ of several independent calibration measurements and corresponds also to the systematic error discussed in Ref. [15].

have performed a combined experimental and theoretical study of lean hydrogen cyanide oxidation in the temperature range of 900–1400 K. The main oxidation route of HCN was found to follow the sequence HCN + OH = CN + H_2O and CN + O_2 = NCO + O. This oxidation sequence is considered by all three mechanisms along with reactions featuring the O and OH radicals. The rate constants in all three mechanisms are similar for most of these reactions. There are, however, two major differences. The present mechanism features the rate for the HCN + O = CN + OH reaction determined by Dean and Bozzelli [26]. This rate is more than one order of magnitude slower than those adopted in the other mechanisms [9, 31]. It may also be noted that the rate constant for the CN + O reaction used in the mechanism of Warnatz et al. [31] is approximately seven times slower than the rates adopted in the present mechanism and GRI-Mech. 2.11.

Results and Discussion

The concentrations of the CH and CN radicals were determined to have maximum values of (1.3 ± 0.5) 10^{12} cm^{-3} and (3.9 ± 1.5) 10^{10} cm^{-3}, respectively. All CH and CN LIF measurements have been performed under linear nonsaturating excitation conditions. This was verified for the strongest transitions of both radicals by plotting the LIF signal intensity versus laser energy, as shown in Fig. 2a. It is important to note that CN (B-X) transitions were found to be saturated at much lower laser energies than the CH (B-X) transitions and, therefore laser energies of less than 1 μJ were chosen in the measurements. For each data point, the laser was scanned over the complete spectral line to account for possible background signals. The N_2 Rayleigh calibration curve is shown in Fig. 2b.

In addition, CH_3 and OH radical concentration profiles are presented in Fig. 3 measured using the *in situ* long-path absorption technique as described in detail by Etzkorn et al. [11]. The OH radical profile was determined from LIF measurements using the A-X (1,0) transition with the absolute calibration being obtained via absorption measurements at the OH A-X (0,0) R-band head around 307 nm (see Etzkorn et al. in Ref. [11]). The relative NO concentration profile shown in Fig. 3 was determined by LIF measurements at the A-X (0,0) transition using the $R_2(21)$ spectral line (see Fitzer in Ref. [11]), and long-path absorption measurements around 225 nm at a height of 38 mm above the burner were used for absolute calibration. The pronounced reduction of NO in the region between 5 and 15 mm above the burner as determined in Ref. [3] could not be reproduced. It was found that the earlier NO measurements were affected by saturation of the NO LIF photomultiplier by the flame emission (see Fitzer in Ref. [11]).

The computed concentration profiles of OH, CH_3, NO, CH, and CN using the different mechanisms are compared with the measured absolute data in Fig. 3. It can be observed that the shape and location of the OH profile is adequately predicted by the three mechanisms in the main reaction zone. There is also excellent agreement between the computed and measured CH_3 profiles. However, the peak CH_3 concentration predicted by GRI-Mech 2.11 is higher than the measurements by ~30%. The initial reduction of NO is well reproduced by the mechanisms. In agreement with the current measurements, the introduction of the NO dopant results in only a minor ~10% reduction in computed CH levels. The CH profile obtained with the mechanism of Warnatz et al. [31] agrees exceptionally well with the experimental results. The predictions using the present mechanism and GRI-Mech 2.11 are higher than the measurements by factors of 1.7 and 2.1, respectively. All three mechanisms overpredict the CN concentrations substantially.

A reaction path analysis reveals both similarities and differences in the modeling of the formation and destruction chemistry of the CH and CN radicals in the three mechanisms. Due to the large amount of molecular oxygen available in the present flame, the consumption of hydrocarbon radicals proceeds to a significant extent via reactions with O_2. The computed CH concentrations are particularly sensitive to the rates of the $^3CH_2 + O_2$, $^3CH_2 + H$, $CH + O_2$, and $CH + H_2O$ reactions. The $^3CH_2 + H$ reaction is the dominant CH formation path in GRI-Mech. 2.11 and the present mechanism. However, this reaction only constitutes a secondary path in the mechanism of Warnatz et al. [31] due to the slower reaction rate adopted as already discussed. The CH radical is primarily formed in the latter mechanism via the reverse of the $CH + H_2O = {}^3CH_2 + OH$ reaction. The computational results using the present mechanism show that the consumption of the CH radical occurs mainly through reactions with O_2 (65%) and H_2O (12%). Although similar peak CH concentrations are predicted by the present mechanism and GRI-Mech. 2.11, the latter mechanism relies on an increased rate (three times) for the $CH + H_2O$ reaction in order to prevent a significant overprediction of CH concentrations. This adjustment was introduced to provide good agreement between simulations using GRI-Mech. 2.11 and measurements of the CH radical made by Luque et al. [13]. However, as discussed by Sick et al. [18], such an increase in the rate of the reaction between CH and H_2O would appear inconsistent with diffusion flame simulations. The present mechanism has also been applied to model the $CH_4/O_2/N_2$ flame measured by Luque et al. [13], and good agreement between the computed (1.7×10^{12} molecules/cm^3) and measured (1.5×10^{12} molecules/cm^3) peak CH concentrations is obtained. This further supports the findings of recent experimental studies [23,35] that the $CH + O_2$ reaction is significantly faster than the CEC recommendation [32]. The present work suggests that a low rate for this reaction constitutes a possible major cause of errors in the computations of CH concentrations in premixed flames. By contrast, the CEC-recommended rate [32] for the $CH + H_2O$ reaction does not appear unreasonable, though product channels evidently remain to be determined at combustion temperatures.

The main differences in the HCN/CN chemistry have been outlined earlier, and the peak HCN concentrations computed by GRI-Mech 2.11 and the Warnatz mechanism are higher than those of the present mechanism by factors of 1.5 and 1.7, respectively. The CN radical is primarily formed from HCN through the hydrogen abstraction reactions and subsequently consumed by the reactions with O_2 and the O and OH radicals. Therefore, the predictions of CN are sensitive to the predictions of the CH and $^3CH_2$ radicals. The measured CN:CH ratio of 1:34 can be compared with the computed values using the present mechanism (1:17), GRI-Mech 2.11 (1:12), and the Warnatz mechanism (1:2.7), respectively. The significant overprediction of CN concentrations obtained with the mechanism of Warnatz et al. [31] is predominantly due to uncertainties in the C atom chemistry and the branching of the NO + CH reaction.

Conclusions

Absolute CH_3, OH, CH, and CN concentrations have been determined in a low-pressure CH_4/O_2 flame seeded with NO using LIF calibrated by Rayleigh scattering. Modeling calculations using three different reaction mechanisms have been shown to produce good agreement for the OH and CH_3 radicals. The amount of NO reduction in the flame is also well predicted. It is further shown that arguably reasonable agreement for the CH and CN profiles may be obtained with the use of recent kinetic data for the dominant reaction channels. However, significant differences in the CH radical formation and destruction chemistry featured in the three mechanisms have been found. The key uncertainties in relation to CH predictions in the present flame have thus been shown to relate to the $^3CH_2 + O_2$, $^3CH_2 + H$, and $CH + H_2O$ reactions. In particular, it is evident that the rate and product distribution for the latter reaction needs to be determined at combustion temperatures. The computational results also show that the quality of predictions for the CN radical is linked with the accurate prediction of the CH radical. The present work also indicates that some uncertainties still prevail in the absolute rate and branching of the CH + NO reaction. Furthermore, it is evident that the C atom chemistry is less well established and may influence computational results significantly. Nevertheless, the agreement obtained between modeling and experiment is encouraging. This work also serves to emphasize the paramount importance of quantitative determinations of key radical species.

Acknowledgments

We would like to thank J. Luque from SRI International for providing the LIFBASE spectral simulation program and V. Sick for helpful discussion. We also would like to thank J. Warnatz for providing his kinetic reaction mechanism. W. Juchmann is funded by the Landesgraduiertenförderung of the Universität Heidelberg. Financial support from the European Union in the framework of the TOPDEC project is gratefully acknowledged.

REFERENCES

1. Thorne, L. R., Branch, M. C., Chandler, D. W., Kee, R. J., and Miller, J. A., in *Twenty-First Symposium (International) on Combustion,* The Combustion Institute, Pittsburgh, 1986, pp. 965–977.

2. Volponi, J. V. and Branch, M. C., in *Twenty-Fourth Symposium (International) on Combustion,* The Combustion Institute, Pittsburgh, 1992, pp. 823–831.
3. Etzkorn, T., Muris, S., Wolfrum, J., Dembny, C., Bockhorn, H., Nelson, P. F., Attia-Shahin, A., and Warnatz, J., in *Twenty-Fourth Symposium (International) on Combustion,* The Combustion Institute, Pittsburgh, 1992, pp. 925–932.
4. Vandooren, J., Branch, M. C., and Van Tiggelen, P. J., *Combust. Flame* 90:247–258 (1992).
5. Zabarnick, S., *Combust. Sci. Technol.* 83:115–134 (1992).
6. Williams, B. A. and Fleming, J. W., *Combust. Flame* 98:93–106 (1994).
7. Williams, B. A. and Fleming, J. W., *Combust. Flame* 100:571–590 (1995).
8. Miller, J. A. and Bowman, C. T., *Prog. Energy Combust. Sci.* 15:287–338 (1989).
9. Frenklach, M., Wang, H., Goldenberg, M., Smith, G. P., Golden, D. M., Bowman, C. T., Hanson, R. K., Gardiner, W. C., and Lissianski, V., Gas Research Institute topical report GRI-95/0058, 1995. http://www.me.berkeley.edu/gri_mech/
10. Lindstedt, R. P., Lockwood, F. C., and Selim, M. N. *Combust. Sci. Technol.* 108:231–254 (1995).
11. Etzkorn, T., Fitzer, J., Muris, S., and Wolfrum, J., *Chem. Phys. Lett.* 208:307–310 (1993); Fitzer, J., "Bestimmung zweidimensionaler Kouzentrations-und Temperaturverteilungen in einer laminaren Niederdruckflamme mit Hilfe der laser induzierlen Fluoreszenzspektroskopie,"Diploma-thesis, University of Heidelberg, 1993.
12. Farrow, R., Bui-Pham, M. N., and Sick, V., in *Twenty-Sixth Symposium (International) on Combustion,* The Combustion Institute, Pittsburgh, 1996, pp. 975–983.
13. Luque, J., Smith, G. P., and Crosley, D. R., in *Twenty-Sixth Symposium (International) on Combustion,* The Combustion Institute, Pittsburgh, 1996, pp. 959–968.
14. Selle, K. and Monkhouse, P., *Appl. Phys. B* 66:645–651 (1998).
15. Luque, J. and Crosley, D. R., *Appl. Phys. B* 63:91–98 (1996); Luque, J., Juchmann, W., and Jeffries, J. B., *Appl. Opt.* 36:3261–3270 (1997).
16. Luque, J. and Crosley, D. R., *LIFBASE: Database and Spectral Simulation Program (Vers. 1.2),* SRI International report MP 96-001, 1996.
17. Jones, W. P. and Lindstedt, R. P., *Combust. Flame* 73:233–249 (1988).
18. Sick, V., Hildenbrand, F. and Lindstedt, R. P., in *Twenty-Seventh Symposium (International) on Combustion,* The Combustion Institute, Pittsburgh, 1998, pp. 1401–1408.
19. Lindstedt, R. P. and Skevis, G., *Combust. Sci. Technol.* 125:75–137 (1997).
20. Lindstedt, R. P., Lockwood, F. C., and Selim, M. N., *Combust. Sci. Technol.* 99:253–276 (1994).
21. Dombrowsky, Ch. and Wagner, H.Gg., *Ber. Bunsen-Ges. Phys. Chem.* 96:1048–1055 (1992).
22. Böhland, T. and Temps, F., *Ber. Bunsen-Ges. Phys. Chem.* 88:459–461 (1984).
23. Markus, M. W., Roth, P., and Just, Th., *Int. J. Chem. Kinet.* 28:171–179 (1996).
24. Grebe, J. and Homann, K. H., *Ber. Bunsen-Ges. Phys. Chem.* 86:587–597 (1982).
25. Dean, A. J., Davidson, D. F., and Hanson, R. K., *J. Phys. Chem.* 95:183–191 (1991).
26. Dean, A. M. and Bozzelli, J. W., in *Combustion Chemistry II* (W. C. Gardiner, Jr., ed.), Springer-Verlag, New York, in press.
27. Bauerle, S., Klatt, M., and Wagner, H. Gg., *Ber. Bunsen-Ges. Phys. Chem.* 99:97–104 (1995).
28. Perry, R. A. and Melius, C. F., in *Twentieth Symposium (International) on Combustion,* The Combustion Institute, Pittsburgh, 1984, pp. 639–646.
29. Wooldridge, S. T., Hanson, R. K., and Bowman, C. T., *Int. J. Chem. Kinet.* 27:1075–1087 (1995).
30. Davidson, D. F., Dean, A. J., DiRosa, M. D., and Hanson, R. K., *Int. J. Chem. Kinet.* 23:1035–1050 (1991).
31. Warnatz, J., Mass, U., and Dibble, R. W., in *Combustion,* Springer-Verlag, New York, 1996, p. 67. Current version: ftp://reaflow.iwr.uni-heidelberg.de/pub/mechanism_for_export/
32. Baulch, D. L., Cobos, C. J., Cox, R. A., Frank, P., Hayman, G., Just, Th., Kerr, J. A., Murrells, T., Pilling, M. J., Troe, J., Walker, R. W., and Warnatz, J., *Combust. Flame* 98:59–79 (1994).
33. Frank, P., Bashkaran, K. A., and Just, Th., *J. Phys. Chem.* 90:2226–2231 (1986).
34. Zabarnick, S., Fleming, J. W., and Lin, M. C., *J. Chem. Phys.* 85:4374–4376 (1986).
35. Röhrig, M., Petersen, E. L., Davidson, D. F., Hanson, R. K., and Bowman, C. T., *Int. J. Chem. Kinet.* 29:781–789 (1997).
36. Berman, M. R., Fleming, J. W., Harvey, A. B. and Lin, M. C., in *Nineteenth Symposium (International) on Combustion,* The Combustion Institute, Pittsburgh, 1982, pp. 73–79.
37. Dean, A. J., Hanson, R. K., and Bowman, C. T., *J. Phys. Chem.* 95:3180–3189 (1991).
38. Glarborg, P. and Miller, J. A., *Combust. Flame* 99:475–483 (1994).

COMMENTS

David M. Golden, SRI International, USA. Comparing the results of the three mechanisms is very interesting. I just want to point out that the GRI-Mech 2.11 mechanism is arrived at by optimizing against several target experiments. Changing one rate constant to agree with one or two new targets, such as your experimental results, may

upset the agreement with other experiments. This is not to say that GRI-Mech should not be improved by a reoptimization. Such reoptimization using new targets and better initial values of the rate constants is a continuing process.

Author's Reply. The adjustment of rate constants in order to bring agreement with experimental data for selected features of a particular flame can indeed be misleading. Such a procedure is naturally subject to the experimental uncertainties inherent in the data, and, furthermore, the multivariate nature of reaction mechanisms typically leads to additional ambiguities. Thus, the intention of the present work has been to assess comprehensively validated reaction mechanisms and independent rate determinations in the context of the measured temperature/species profiles. Mechanism development is certainly a continuing process, and it is suggested that any future reoptimization of the GRI mechanism may tentatively consider a rebalancing of the CH chemistry in favor of measured rates for the CH + O_2 (Refs. [23,35] in the paper), CH + H_2O [1], and CH + N_2 [2] channels [3]. However, we would also like to draw attention to the need for further validation data and independent determinations of rates and product distributions for the key reaction channels.

REFERENCES

1. Zabarnick, S., Fleming, J. W., and Lin, M. C., in *Twenty-First Symposium (International) on Combustion,* The Combustion Institute, Pittsburgh, 1986, pp. 713–719.
2. Dean, A. J., Hanson, R. K., and Bowman, C. T., in *Twenty-Third Symposium (International) on Combustion,* The Combustion Institute, Pittsburgh, 1990, pp. 259–265.
3. Sick, V., Hildenbrand, F., and Lindstedt, R. P., in *Twenty-Seventh Symposium (International) on Combustion,* The Combustion Institute, Pittsburgh, 1998, pp. 1401–1408.

•

S. Cheskis, Tel Aviv University, Israel. When comparing absolute concentration measurements with calculation results, the uncertainties in temperature measurements must also be taken into account. Temperature values are needed both for model calculation and for processing of the experimental data. Could you estimate the total uncertainty in the comparison of your experimental results with theoretical predictions?

Author's Reply. The experimental uncertainty in temperature of ±50 K influences the Boltzmann factor and the overlap factor by less than 8%. For the modeling calculations, an analytical expression was fitted to the experimental temperature profile and used for the calculations. Therefore, the calculated profiles do not reflect the uncertainties in the experimental temperature profile. Calculations in the same flame showed that a variation of temperature of ±50 K leads to changes in the CH and CN profiles of 5–7%.

•

Jay Jeffries, SRI International, USA. In our experience, low-pressure flames below 20 Torr are inflamed by radical transport and are not described well with a 1-D transport model. This problem is greater in O_2 flames than in air flames. For your 10-Torr methane/air flame, would you comment on the possible effects of radical expansion. I would expect radical transport to slow the gas velocity, allowing more reaction time at each point in the temperature profile above the burner. I expect this to lower the predicted CH concentration.

Author's Reply. Two-dimensional LIF measurements of OH and NO in the same flame have been performed in Ref. [11b] in the paper. They show that the expansion of the gas flow is marginal. Reaction models that describe the combustion process in two dimensions will be able to cope with the effects of area expansion and have recently be developed in Heidelberg. Pseudo 2-D codes, which vary the gas velocity with the distance above the burner, might be an alternative to full 2-D models. However, for these models, it is critical to determine how much the gas velocity changes with the distance above the burner.

•

John W. Daily, University of Colorado at Boulder, USA. What is the uncertainty in your CH and CN measurements?

Author's Reply. The statistical error of several independent measurements was determined to be 38%, which is slightly higher than the systematic error for CH (Ref. [15] in the paper). However, the systematic error for CN is larger than for CH, because the radiative lifetime of CN is a factor of 6 lower than the radiative lifetime of CH, therefore increasing the error for the quenching correction to 5% and the overall error to 42%.